Surface Properties of Hydrous Manganite (γ-MnOOH). A Potentiometric, Electroacoustic, and X-ray Photoelectron Spectroscopy Study

ARTICLE *in* LANGMUIR · SEPTEMBER 2004

Impact Factor: 4.46 · DOI: 10.1021/la0496338 · Source: PubMed

4 AUTHORS:

Madeleine Ramstedt
Umeå University
37 PUBLICATIONS **597** CITATIONS
SEE PROFILE

Britt Andersson
Umeå University
39 PUBLICATIONS **488** CITATIONS
SEE PROFILE

Andrey Shchukarev
Umeå University
108 PUBLICATIONS **1,398** CITATIONS
SEE PROFILE

Staffan Sjöberg
Umeå University
170 PUBLICATIONS **4,386** CITATIONS
SEE PROFILE

Surface Properties of Hydrous Manganite (γ-MnOOH). A Potentiometric, Electroacoustic, and X-ray Photoelectron Spectroscopy Study

Madeleine Ramstedt,*,† Britt M. Andersson,‡ Andrei Shchukarev,† and Staffan Sjöberg†

Department of Chemistry, Inorganic Chemistry, and Department of Applied Physics and Electronics, Umeå University, SE-901 87 Umeå, Sweden

Received February 11, 2004. In Final Form: June 24, 2004

The acid−base characteristics of the manganite (γ-MnOOH) surface have been studied at pH above 6, where dissolution is negligible. Synthetic microcrystalline particles of manganite were used in the experiments. From potentiometric titrations, electrophoretic mobility measurements, and X-ray photoelectron spectroscopy (XPS), a one pK_a model was constructed that describes the observed behavior. The data show no ionic strength effect at pH < 8.2, which is the pH at the isoelectric point (pH_{iep}), but ionic strength effects were visible above this pH. To explain these observations, Na^+ ions were suggested to form a surface complex. The following equilibria were established: $\equiv MnOH_2^{+1/2} \rightleftharpoons \equiv MnOH^{-1/2} + H^+$, log β^0 (intr.) = −8.20; $\equiv MnOH_2^{+1/2} + Na^+ \rightleftharpoons \equiv MnOHNa^{+1/2} + H^+$, log β^0 (intr.) = −9.64. The excess of Na^+ at the surface was supported by XPS measurements of manganite suspensions containing 10 mM NaCl. The dielectric constant of synthetic manganite powder was also determined in this study.

Introduction

Mineral surfaces are important in environmental processes regulating both the mobility and speciation of metals and inorganic/organic ligands. Important information for prediction of adsorption processes is the charge and acid−base properties of the pure surface but also the dissolution of the mineral surface. It is well-known that anions tend to adsorb more strongly to a positively charged surface (i.e., a surface at pH below the pH of point of zero charge (pH_{pzc})) while cations preferentially adsorb at higher pH where the surface is less positive or negatively charged. Several types of naturally occurring secondary minerals, such as the oxides and hydroxides of Fe, Al, and Mn, are important surfaces in this perspective. One of these, manganite (γ-MnOOH), is the focus of the present study. Manganite has been reported to be present in lakes and rivers in the temperate and subarctic zones of the world,[1−4] and thus, it should play an important role in the geochemical cycling of elements in these areas.

Although manganite might be an important constituent of natural waters, it has not been studied to the same extent as, e.g., many iron (hydr)oxides. Previous studies largely deal with the redox sensitivity of manganite, which oxidizes organic material such as oxalate,[5] ascorbic acid,[6] aromatic compounds,[7] and aminocarboxylates,[8] as well as metal ions such as As(III)[9] and Cr(III),[10] while reducing Pu(VI).[11] In addition to these studies, there are a few adsorption studies of metals which are not redox sensitive, e.g., Pb(II),[12] Cd(II),[13] and Zn(II).[14,15] Only one publication exists in which the acid−base properties of manganite have been described,[5] which reports two protolysis constants, $pH_{a1}^{int} = 5.72$ and $pK_{a2}^{int} = 6.66$, and the pH_{pzc} at pH 6.2. Apart from this, few other determinations of pH_{pzc} also exist,[5,11,12,16] but the disagreement between these studies calls for further investigation.

The objective of this study was to describe the surface charge and acid−base properties of manganite in the pH range beyond the onset of dissolution[17] (i.e., above pH 6) and also to determine the dielectric constant of manganite. The dissolution of manganite at low pH has been reported previously[17] and will be described more in detail in a forthcoming publication.[18]

* To whom correspondence may be addressed: Phone: +46 (0)90 786 9635. Fax: +46 (0)90 786 9195. E-mail: madeleine.ramstedt@chem.umu.se.

† Department of Chemistry, Inorganic Chemistry.

‡ Department of Applied Physics and Electronics.

(1) Crerar, D. A.; Cormick, R. K.; Barnes, H. L. In *Geology and Geochemistry of Manganese Vol 1. Mineralogy, Geochemistry, Methods*; Varentsov, I. M., Grasselly, G. Y., Eds.; E. Schweizerbart'sche Verlagsbuchhandlung: Stuttgart, 1980.

(2) Hem, J. D.; Lind, C. J. *Geochim. Cosmochim. Acta* **1983**, *47*, 2037−2046.

(3) Stumm, W.; Giovanoli, R. *Chimia* **1976**, *30* (6), 423−425.

(4) Murray, J. W.; Dillard, J. G.; Giovanoli, R.; Moers, H.; Stumm, W. *Geochim. Cosmochim. Acta* **1985**, *49*, 463−470.

(5) Xyla, A. G.; Sulzberger, B.; Luther, G. W.; III; Hering, J. G.; Van Cappellen, P.; Stumm, W. *Langmuir* **1992**, *8*, 95−103.

(6) Shin, Y.; Martin, S. T. *Environ. Sci. Technol.* **2003**, *37*, 2363−2370.

(7) Zhang, H.; Huang, C. *Environ. Sci. Technol.* **2003**, *37*, 2421−2430.

(8) Mcardell, C. S.; Stone, A. T.; Tian, J. *Environ. Sci. Technol.* **1998**, *32*, 2923−2930.

(9) Chiu, V. Q.; Hering, J. G. *Environ. Sci. Technol.* **2000**, 34, 2029−2034.

(10) Johnson, C. A.; Xyla, A. G. *Geochim. Cosmochim. Acta* **1991**, *55*, 2861−2866.

(11) Shaughnessy, D. A.; Nitsche, H.; Booth, C. H.; Shuh, D. K.; Waychunas, G. A.; Wilson, R. E.; Gill, H.; Cantrell, K. J.; Serne, R. J *Environ. Sci. Technol.* **2003**, *37*, 3367−3374.

(12) Matocha, C. J.; Elzinga, E. J.; Sparks, D. L. *Environ. Sci. Technol.* **2001**, *35*, 2967−2972.

(13) Bochatay, L.; Persson, P.; Sjöberg, S. *J. Colloid Interface Sci.* **2000**, *229*, 584−592.

(14) Bochatay, L.; Persson, P. *J. Colloid Interface Sci.* **2000**, *229*, 593−599.

(15) Pan, G.; Qin, Y.; Li, X.; Hu, T.; Wu, Z.; Xie, Y. *J. Colloid. Interface Sci.* **2004**, *271*, 28−34.

(16) Weaver, R. M.; Hochella, M. F.; Ilton, E. S. *Geochim. Cosmochim. Acta* **2002**, *66* (23), 4119−4132.

(17) Ramstedt, M.; Shchukarev, A. V.; Sjöberg, S. *Surf. Interface Anal.* **2002**, *34*, 632−636.

(18) Ramstedt, M.; Sjöberg, S. Low pH Phase Transformation and Proton Promoted Dissolution of Hydrous Manganite (γ-MnOOH). Manuscript in preparation.

10.1021/la0496338 CCC: $27.50
Published on Web 08/10/2004

Methods and Experimental Section

In this work a number of different methods were used in order to determine the acid−base characteristics of manganite. The synthesized manganite powder was characterized using X-ray powder diffraction (XRD), scanning electron microscopy (SEM), and high-resolution transmission electron microscopy (HR-TEM) to confirm the crystallinity and purity of the phase formed. The surface area was determined using the BET method.

To investigate surface charging, the AcoustoSizer technique was used and the dielectric constant was determined to be used in the calculation of surface potentials in the AcoustoSizer software. X-ray photoelectron spectroscopy (XPS) was used to follow the changes in surface composition with pH, and potentiometric titrations were performed to determine an acid−base model for the surface.

Solutions and Suspensions. All solutions were made from deionized and boiled water (Milli-Q Plus 185) at ionic strengths of 0.01, 0.03, and 0.1 M NaCl (Merck p.a., dried at 180 °C). Stock solutions of HCl (Fisher, p.a.) were standardized against tris(hydroxymethyl)aminomethane (Trizma base). NaOH (Merck, p.a.) solutions were standardized against the above-mentioned standardized H^+ solutions. Standard solutions of Mn^{2+} were prepared from $MnCl_2 \cdot 4H_2O$ (Merck p.a.) and were standardized against a Mn(II) solution of known concentration obtained by dissolution of Mn metal. Atomic absorption spectrometry was used to ensure the absence of dissolution, i.e., aqueous manganese, at pH > 6.

Manganite was synthesized, by adding 300 mL of 0.2 M NH_3 (Merck p.a.) to a solution of 20.4 mL of 30% H_2O_2 (JT Baker p.a.) and 1 L of 0.06 M $MnSO_4$ (BDH).[17,19] The mixture was heated and kept at a temperature of 95 °C for 6 h under constant stirring with a magnetic stirrer. The suspension was subsequently filtered while hot through a G4 glass filter, washed with an equal amount (with respect to the initial solution) of hot deionized water, and dried under reduced pressure in the presence of P_2O_5 (Riedel-de Haën). The dried manganite was ground to a powder and the purity checked using X-ray powder diffraction. In the diffraction patterns only the typical *d* spacings for manganite at 3.41, 2.64, 2.52, 2.41, 2.20, 1.78, 1.70, 1.67, 1.50, 1.44, and 1.32 Å were found. The manganite was stored as a powder, from which suspensions with known amounts of solid were prepared and put in an ultrasonic bath for a few minutes to disperse the particles. The suspensions were thoroughly bubbled with Ar(g) at the time of preparation and before the potentiometric titrations. Typically, 10 g of manganite were used per liter of suspension, except for the AcoustoSizer measurements, where 20 g of manganite was used per liter of suspension. The manganite crystals dispersed well in suspensions, although they formed aggregates when dried.

The surface area of manganite was experimentally determined using the BET method with degassing at 70 °C, to prevent phase transformations.[13] The BET area was 51 m^2/g for the manganite batch used in the titrations and 39 m^2/g for the batch used in the AcoustoSizer measurements. The differences in surface area between different batches of manganite have previously been ascribed to a size difference between the needles synthesized.[19] The manganite crystals synthesized here were needle shaped with an average length of approximately 500 nm and width of about 40 nm. Thus, the theoretical surface area for a cylindrical crystal would be 24 m^2/g, while a box-shaped crystal with the dimensions of 40 × 20 × 500 nm would correspond to a surface area of 36 m^2/g (using a manganite density[20] of 4.3 g/cm^3). When these theoretical calculations of the surface area were compared with the experimental BET measurements (39 m^2/g), it seems as if the needles have a smaller height than width, i.e., are not completely cylindrical but oval or rectangular in cross section. However, this difference can also be due to an overestimation of the average needle dimensions. From SEM pictures, the needles appear somewhat flattened, and also the presence of smaller needles can be seen (Figure 1a). The crystallinity was confirmed using HR-TEM, which shows a highly ordered atomic structure of the manganite needles (Figure 1b).

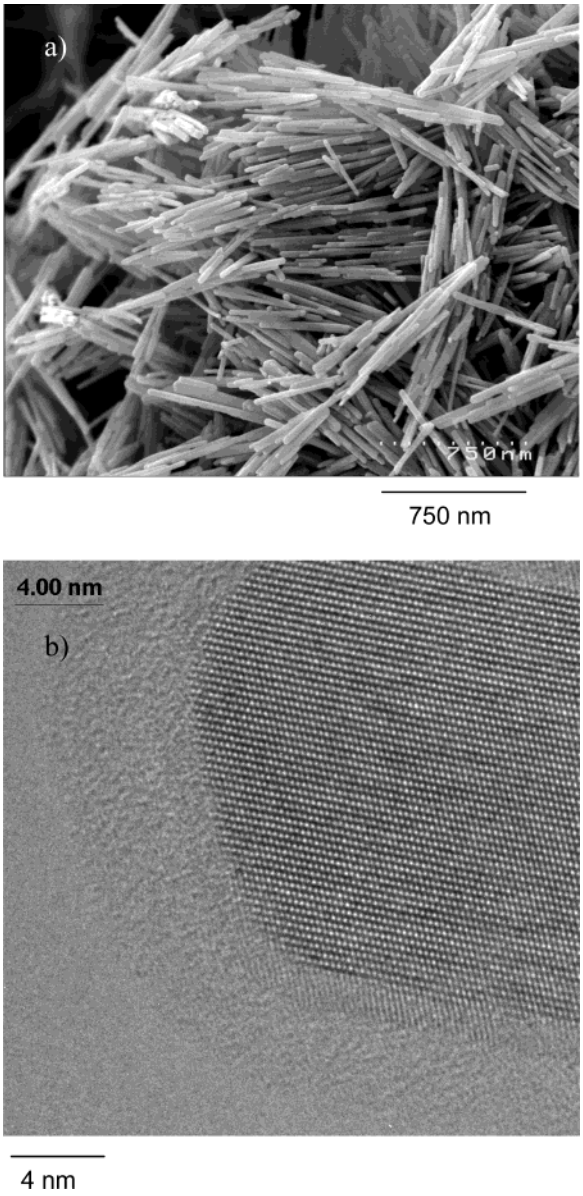

Figure 1. (a) SEM picture of manganite crystals. The scale bar represents 750 nm. (b) TEM picture showing one end of a manganite crystal. The scale bar represents 4 nm.

Manganite suspended in a pure aqueous solution typically gives a pH of around 6, which is below pH of the isoelectric point (pH_{iep}) (discussed in later paragraphs). This implies that anions must be present at the surface to balance the positive charge. In the synthesis, manganese sulfate is used as starting material and, consequently, it can be anticipated that sulfate would be the anion found at the surface. To determine this concentration of sulfate, pH was increased to over 11 in an aliquot of the suspension. This aliquot was left to equilibrate for several days, after which the suspension was centrifuged and the concentration of sulfate in the filtered solution was determined using ion chromatography. In 10 g/L suspensions, 0.14 ± 0.01 mM sulfate was found, which would correspond to a positive surface charge formed by 0.28 ± 0.02 mM H^+ or 0.55 ± 0.04 μmol of H^+/m^2.

The crystal structure of manganite consists of Jahn−Teller elongated Mn(III)−O_6 octahedra arranged in a rutile-type structure[21,22] (Figure 2). At the surface, it can be expected that singly coordinated oxygens will be the most reactive due to their position and their relatively high charge. The singly coordinated oxygens will display a formal charge of $-1/2$ if deprotonated,

(19) Giovanoli, R.; Leuenberger, U. *Helv. Chim. Acta* **1969**, *52* (8), 2333−2347.
(20) Garrido, M. J. *Bull. Soc. Fr. Mineral.* **1935**, *58*, 224−241.
(21) Buerger, M. J. *Z. Kristallogr.* **1936**, *95*, 163−174.
(22) Kohler, T.; Armbruster, T. *J. Solid State Chem.* **1997**, *133*, 486−500.

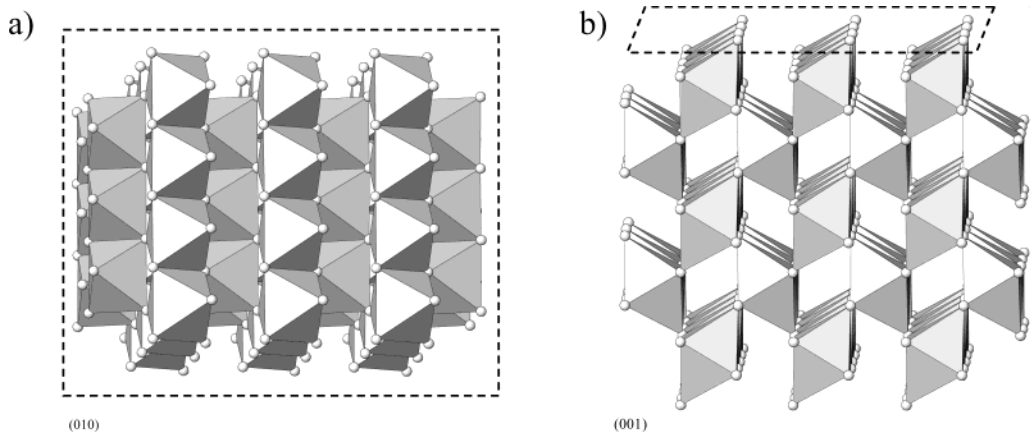

Figure 2. The crystal structure of manganite (Buerger[21]). The dotted lines show the position of the (010) plane. In part a the (010) plane of the structure is in the plane of the paper, and in part b the (001) plane of the structure is in the plane of the paper. Hydrogens are omitted for clarity.

or $+^1/_2$ if protonated (1), according to Pauling's valence bond theory.[23]

$$\equiv MnOH^{-1/2} + H^+ \rightleftharpoons \equiv MnOH_2^{+1/2} \quad (1)$$

Assuming that the surface will display the same structure as the bulk, a theoretical number of sites can be estimated from specific planes of the crystals. The dominating planes for small manganite crystals have not been determined and may differ compared to larger crystals.[24] However, we assume that the small manganite crystals synthesized in this study are dominated by the (010) plane since this plane has been shown to be predominant in large manganite crystals and constitutes a plane of cleavage.[25] The (010) plane hosts 7.9 sites/nm^2, which also is approximately the site concentration for other dominating planes on large manganite crystals.

Only one experimental study of the density of sites has been reported for manganite. This fluoride adsorption study cited by Xyla[5] resulted in 5 sites per nm^2. In the present study, attempts to determine the number of surface proton active sites utilizing the potentiometric titration technique failed. No saturation level with respect to surface proton uptake could be observed due to the onset of dissolution at low pH.[17]

Dielectric Constant Determination. To determine the dielectric constant, manganite powder was pressed at room temperature to pellets with a diameter of 45 mm and a thickness of 1.5 mm. A pressure of 8.0 MPa was applied during this process by the use of an isostatic hydraulic press. To certify that no phase transitions took place, X-ray powder diffraction studies of the material were performed before and after the measurements. The pellets were placed between metal electrodes, and the capacitance was measured at room temperature as a function of frequency, using a frequency response analyzer, Solitron 1260. The dielectric constant was derived from the measured capacitance, the surface area, and the thickness. The dimensions of the pellets were determined with accuracy better than 0.2% for the area and 0.6% for the thickness. The frequency was varied from 100 Hz to 1 GHz.

The dielectric constant decreases as the frequency is increased and, hence, shows a typical characteristic of normal dielectrics. The measured effective dielectric constant for the pressed sample was 6.4 at 10 kHz and 3.7 at 1 MHz. Since the frequencies in the AcoustoSizer measurements lie in the megahertz range, the latter value for the dielectric constant was used for calculations of surface potentials in the AcoustoSizer software.

To account for the porosity of the samples, and to derive the dielectric constant for the individual γ-MnOOH crystals, a so-called mixing model can be applied. This model depicts the crystal powder as a mixture of capacitors in series or parallel connection. Different mixing models predict different values, but there are bounds that limit the range of the predictions. The loosest bounds, following the effective medium theory, are the so-called Wiener bounds.[26] These predict the lowest value of the crystals to be about 10 at 1 MHz. The lower bound assumes that the crystals and the air gap between them are entirely connected in parallel. A more realistic model would contain a mixture of parallel and series connections. For this, the commonly used Looyenga formula[27] predicts a dielectric constant of 24 and the Maxwell Garnett mixing rule[28] a value of 16 for the crystals, both at 1 MHz.

X-ray Photoelectron Spectroscopy. To obtain information about the surface composition, XPS spectra were collected with a KRATOS Axis Ultra electron spectrometer under monochromatic Al Kα radiation (1486.6 eV). A pass energy of 160 eV with a step size of 1 eV was used for survey scans. For separate photoelectron lines, a pass energy of 10 eV was used with a step size of 0.1 eV. To compensate for the charging of the surface, charge neutralizing equipment was used and the binding energy (BE) scale was referenced to the adventitious C 1s peak at 285.0 eV. The typical carbon contamination at the surface was less than 5 atom %. The samples were analyzed as frozen pastes ($T < -155$ °C) in order to keep the water−mineral interface as intact as possible since it has been shown that a loss of water at the interface can change the chemical speciation of adsorbed species.[29] All XPS samples were prepared from suspensions containing an ionic strength (NaCl) of 10 mM. The pH values of ~10 mL aliquots of the stock suspension were adjusted using NaOH or HCl solutions. After equilibrating for approximately a week, a sample was centrifuged and the wet manganite paste was applied onto a sample holder. The sample holder was placed onto a precooled transfer rod (−170 °C) of the spectrometer where it was quickly frozen. The introducing chamber was then evacuated, and the sample was introduced into the analysis chamber. The temperature of the sample was kept at approximately −155 °C, or below, throughout the entire measurement. In all analyses, the pressure in the analysis chamber was below 10^{-8} Torr.

AcoustoSizer. Measurements to determine the pH of the isoelectric point (pH_{iep}) were performed using the electroacoustic technique developed by O'Brien.[30] The AcoustoSizer was calibrated with a silica suspension and background corrections were performed using solutions containing only ionic media. The AcoustoSizer measurements were performed on manganite suspensions of 0.46 vol % (20 g/L). The suspension was stirred

(23) Pauling, L. *J. Am. Chem. Soc.* **1929**, *51*, 1010−1026.
(24) Rakovan, J.; Becker, U.; Hochella, M. F., Jr. *Am. Mineral.* **1999**, *84*, 884−894.
(25) Berry, L. G.; Mason, B. *Mineralogy—Concepts, descriptions, determinations*, 2nd ed.; Dietrich, R. V. W. H., Ed.; Freeman and Company: San Fransisco, CA, 1983; pp 318−319.
(26) Wiener, O. *Abh. Leipz. Akad.* **1912**, *32*, 509.
(27) Looyenga, H. *Physica* **1965**, 31, 401−406.
(28) Kärkkäinen, K. K.; Sihvola, A. H.; Nikoskinen, K. I. *IEEE Trans. Geosci. Remote Sensing* **2000**, *38* (3), 1303−1308.
(29) Ramstedt, M.; Nordgren, C.; Sheals, J.; Shchukarev, A.; Sjöberg, S. *Surf. Interface Anal.*, in press.
(30) O'Brien, R. W.; Cannon, D. W.; Rowlands, W. N. *J Colloid Interface Sci.* **1995**, *173*, 406−418.

with a propeller (450−600 rpm) during the measurements. The pH was measured with a combination electrode calibrated with commercial pH buffers. NaOH was added to the suspension to obtain different pH values. After each addition of NaOH, the suspension was left to equilibrate for at least 15 min.

Within the software of the commercially available AcoustoSizer instrument, the experimentally determined electrophoretic mobility is recalculated into zeta potential and particle size. This zeta potential corresponds to the potential at the slip plane of the particle−solution interface. The dielectric constant of manganite does not affect the calculated surface potential since it is lower than the dielectric constant for water (78 at 25 °C[31]). Further details regarding the theory behind the electroacoustic technique can be found in O'Brien et al.[30]

Potentiometric Titrations. Surface speciation and equilibria in the γ-MnOOH−H^+−Na^+−Cl^- system were determined by potentiometric titrations at 25.00 ± 0.05 °C. The experiments were performed with an automatic system for precise potentiometric titrations designed and built at our department.[32] The cell arrangement, immersed in an oil thermostat, was similar to that described by Forsling et al.[33] To avoid activity coefficient variations, a constant ionic medium of 0.1 or 0.03 M Na(Cl) was used. The free H^+ concentration was determined by measuring the emf (E) of the cell:

−Ag, AgCl(s)|ionic medium (0.1 or 0.03 M NaCl)||
equilibrium solution|glass electrode+

The response of the electrode is given by the Nernst equation (E in mV)

$$E = E_0 + g \log[H^+] + E_j \quad (2)$$

E_0 (in mV) is an apparatus constant for the cell. It is determined from separate titrations of a hydrochloric acid solution with known concentration, immediately before and after the manganite titrations and in the respective ionic media. The difference in E_0 between subsequent measurements was always smaller than 2 mV. The parameter $g = RT \ln 10/(nF) = 59.16$ mV (R = molar gas constant (8.314 J mol^{-1} K^{-1}), T = temperature (K), n = number of electrons, here $n = 1$, and F = Faraday's constant (96485 C mol^{-1})) at 25 °C, and E_j (in mV) is the liquid junction potential at the interface between the solution and the salt bridge, generally expressed as

$$E_j = j_{ac}[H^+] + j_{alk}K_W[H^+]^{-1} \quad (3)$$

In eq 3, K_W is the autoprotolysis constant of water and j_{ac} and j_{alk} are constants that influence E_j in acidic and alkaline conditions, respectively. For 0.1 M NaCl the following values are valid,[34] $j_{ac} = -511.5$ mV M^{-1}, $j_{alk} = 238.7$ mV M^{-1}, and $K_w = 10^{-13.75}$ M^2, and for 0.03 M NaCl, $j_{ac} = -1656$ mV M^{-1}, $j_{alk} = 713.3$ mV M^{-1}, and $K_w = 10^{-13.87}$ M^2. In the presence of manganite, a drift in the recorded potential of less than 0.1 mV per hour was usually reached within 60−120 min after each addition of base, and at that time the next addition of base was made. In the separate acid−base titrations to determine E_0, stable potentials were usually reached in less than 10 min. To produce the best reproducibility in the acid−base titrations of manganite suspensions, it was observed that the stock suspension should be allowed to age for a couple of months before performing the potentiometric titrations.

Experimentally determined −log[H^+] values were recalculated to pH values by calculating activity coefficients (γ) according to Davies equation[35] (4) where I is the ionic strength in (M).

$$\log \gamma(H^+) = -0.509\left(\frac{I^{1/2}}{1 + I^{1/2}} - 0.3I\right) \quad (4)$$

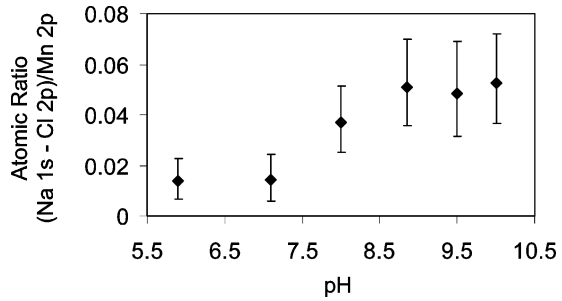

Figure 3. Relative concentration of excess Na^+ at the manganite surface at different pH (from suspensions containing 10 mM NaCl). The concentration ratio (Na 1s − Cl 2p)/Mn 2p corrects for Na^+ present as a NaCl precipitate and for differences in water content. Error bars represent a 10% error in atomic concentrations.

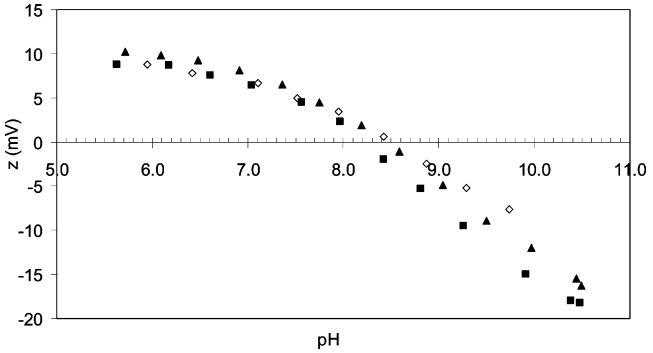

Figure 4. Experimentally determined potentials at the shear plane of manganite at three different ionic strengths: ■ = 10 mM NaCl, ▲ = 30 mM NaCl, and ◇ = 100 mM NaCl.

Experimental data were modeled using a modified version (J. Lützenkirchen, personal communication) of the computer program Fiteql2.[36]

Results and Discussion

Surface Composition. The chemical composition of the surface was studied by XPS, as previously described.[17] In short, the changes in concentration of Na^+, Cl^-, and OH groups were measured as a function of pH. The relative concentration of OH groups increased with pH, and this was explained as due to the deprotonation of surface $\equiv MnOH_2^{+1/2}$ groups according to reaction 1. Furthermore, a small excess of Na^+ at the surface was found at pH ≥ 7.8, as is shown in Figure 3, indicating an interaction between the negatively charged surface groups and the Na^+ ions.

Surface Charge Properties. To indirectly measure the charging of the manganite surface, the surface potential of the crystals was examined at different ionic strengths and pH values using the AcoustoSizer technique. The potential of the manganite surface was low in the pH range between 6 and 8 (Figure 4), compared to, e.g., goethite.[37] Goethite displays potentials of up to 50 mV in this pH range, while the manganite potentials never rise above 10 mV. Furthermore, no significant ionic strength dependence could be seen in this pH range; i.e., the data at the three ionic strengths more or less overlapped within

(31) Atkins, P. W. *Physical Chemistry*, 5th ed.; Oxford University Press: Oxford, 1994.
(32) Ginstrup, O. *Chem. Instrum.* **1973**, 141−155.
(33) Forsling, W.; Hietanen, S.; Sillén, L. G. *Acta Chem. Scand.* **1952**, *6*, 901.
(34) Sjöberg, S.; Hägglund, Y.; Nordin, A.; Ingri, N. *Mar. Chem.* **1983**, *13*, 35−44.
(35) Davies, C. W. *Ion Association*; Butterworths: London, 1962.
(36) Westall, J. C. FITEQL: *A Computer Program for Determination of Chemical Equilibrium Constants from Experimental Data*, Version 2.0, Report 82-02; Department of Chemistry, Oregon State University: Corvallis, OR, 1982.
(37) Boily, J.-F.; Lützenkirchen, J.; Balmès, O.; Beattie, J.; Sjöberg, S. *Colloids Surf., A* **2001**, *179*, 11−27.

Table 1. Literature Data for pH_{pzc}/pH_{iep}

	surface area[a]	pH_{pzc}/pH_{iep}	method	MnOOH origin
Weaver et al.[16]	8.9	5.4	titration	natural
Shaughnessy et al.[11]	9.5	7.4	titration	natural
Xyla et al.[5]	30.5	6.2	titration	synthetic
Matocha et al.[12]	32	6.3	em[b]	synthetic
this study	39	8.5	em (I = 100 mM)	synthetic
	39	8.2	em (I = 10 mM)	synthetic
	51	8.2	estimation from BE shifts in XPS	synthetic

[a] Surface area in m^2/g. [b] em = electrophoretic mobility.

the experimental uncertainties (estimated to ±1 mV). The isoelectric point was recorded at pH 8.2 ± 0.1 in 10 mM NaCl with a small shift to higher pH at the higher ionic strengths, which could indicate some surface interaction with Na^+ from the ionic medium. In the pH range above the pH_{iep}, a more pronounced ionic strength dependence was indicated, again suggesting that the electrolyte ions (i.e., Na^+) are not indifferent or that they have different affinity for the surface in the vicinity of pH_{iep}.

An indirect method for determining pH_{pzc} by using XPS measurements was proposed by Cattania et al.[38] It involves estimating the acid−base behavior of the oxide surface from the metal acidity and oxygen basicity. In this approach, the pH_{pzc} is calculated using the chemical shifts of different components in manganite together with the linear relationship shown in eq 5 (where BE is the binding energy of the component in question).

$$pH_{pzc} = 11.32 - 1.14((BE_{O1s\ oxide} - 530.0) + (BE_{cation} - BE_{metal})) \quad (5)$$

Since the Mn 2p peak has a complicated substructure,[39] the BE for the highest region on $2p_{3/2}$ was chosen as BE for the mineral (BE_{cation} = 641.9 eV). The BE value for Mn(s) was obtained from Moulder et al.[40] (BE_{metal} = 639.0 eV) and $BE_{O1s\ oxide}$ was measured to 529.8 eV. With this approach, the calculated pH_{pzc} of manganite is calculated to be at pH 8.2, i.e., very close to the experimentally determined pH_{iep}.

Table 1 shows large discrepancies in the different pH_{pzc}/pH_{iep} for different manganite materials reported in the literature. However, there are difficulties concerning the correct determination of pH_{pzc} from titrations since the charge of the surface is not always equal to zero in the starting material. Consequently, techniques using electrophoretic mobility are generally more reliable for determining $pH_{pzc/iep}$ providing surface impurities are negligible.

Acid−Base Properties. Potentiometric titrations of the suspension showed a low buffer capacity (≈10^{-5} M g^{-1} pH^{-1}) at pH < 7.5. Furthermore, no or very little ionic strength dependence was observed in accordance to the zeta-potential measurements. At higher pH, the buffer capacity increased with increasing ionic strength, which can be explained by Na^+ interactions with the surface (eq 6) and is in agreement with previous XPS-measurements (see above).

$$\equiv MnOH_2^{+1/2} + Na^+ \rightleftharpoons \equiv MnOHNa^{+1/2} + H^+ \quad (6)$$

(38) Cattania, M. G.; Aridizzone, S.; Bianchi, C. L.; Carella, S. *Colloids Surf., A* **1993**, *76*, 233−240.
(39) Gupta, R. P.; Sen, S. K. *Phys. Rev. B* **1975**, *12*, 15−19.

Table 2. Modeling Parameters and Results[a]

	CCM
capacitance (F/m^2), C	*0.39*
B_0 (μmol/m^2)[b]	13
H_0 (μmol/m^2)[b]	0.55
surface area (m^2/g)	51
log $\beta^0_{1,-1,0}$ (intr.)	−8.20
log $\beta^0_{1,-1,1}$ (intr.)	*−9.64 ± 0.01*

The constants are defined according to the following equilibrium: $\equiv MnOH_2^{+1/2} + qH^+ + rNa^+ \rightleftharpoons \equiv MnOH_{2+q}Na_r^{(+1/2+q+r)}$; $\beta_{1,q,r}$. Parameters in italics have been varied during the modeling. [b] H_0 = total concentration of H^+ in the suspension at the start of titration, as determined from sulfate analysis, and B_0 = density of crystallographic surface sites.

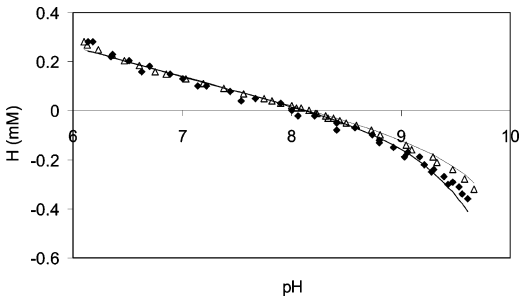

Figure 5. Potentiometric titration data for manganite suspensions with 100 mM NaCl (◆) and 30 mM NaCl (△) ionic medium. The solid lines represent the model with parameters from Table 2.

The pH at the net zero proton condition (pH_{nzpc}) was determined to be 8.1 ± 0.1 at the two ionic strengths studied (100 and 30 mM), and this is in agreement with pH_{iep} within the experimental uncertainties.

The strategy of the equilibrium analysis was to explain the experimental datasets with a model containing as few adjustable parameters as possible. This implied that ionic strength effects (mainly Na^+ effects) had to be accounted for at high pH but not at low pH. Since the constant capacitance model (CCM[41]) does not consider ionic strength effects and the basic Stern model (BSM[42]) gives ionic strength effects both at low and at high pH, neither of these models were applicable. Hence, the ionic strength dependence observed here was modeled by considering a surface complex between Na^+ and the negatively charged sites on the surface. The one-pK model introduced by Bolt and van Riemsdijk[43,44] was used, and the proton affinity constant was set equal to the pH_{iep} obtained from the electroacoustic measurements. Since pH_{iep} has a slight dependence on ionic strength (Na^+ concentration), the value of pH_{iep} = 8.2 from data at 0.01 M NaCl was used since it is closest to zero ionic strength. This value is also equal to pH_{nzpc} within the experimental errors (cf. Figure 4). The model applied contains only two adjustable parameters, the capacitance C and the affinity constant for the Na^+ interaction with the surface. The results are presented in Table 2, and the fit of calculated proton data to experimental data is visualized in Figure 5.

As can be seen from Figure 5, the fit is surprisingly good considering the very simple model applied. Diagrams

(40) Moulder, J. F.; Stickle, W. F.; Sobol, P. E.; Bombem, K. D. *Handbook of X-ray Photoelectron Spectroscopy*; Chastain, J., King, R. C., Jr., Eds.; Physical Electronics Inc.: Chanhassen, MN, 1995.
(41) Schindler, P. W.; Gamsjäger, H. *Kolloid Z. Z. Polym.* **1972**, *250*, 759−765.
(42) Lützenkirchen, J.; Boily, J. F.; Sjöberg, S. *Curr. Top. Colloid Interface Sci.* **2002**, *5*, 157−190.
(43) Bolt, G. H. In *Soil Chemistry, B. Physico-Chemical Models*; Elsevier: Amsterdam, 1982; Chapter 13.
(44) Van Riemsdijk, W. H.; Bolt, G. H.; Koopal, L. K.; Blaakmeer, J. *J. Colloid Interface Sci.* **1986**, *109*, 219.

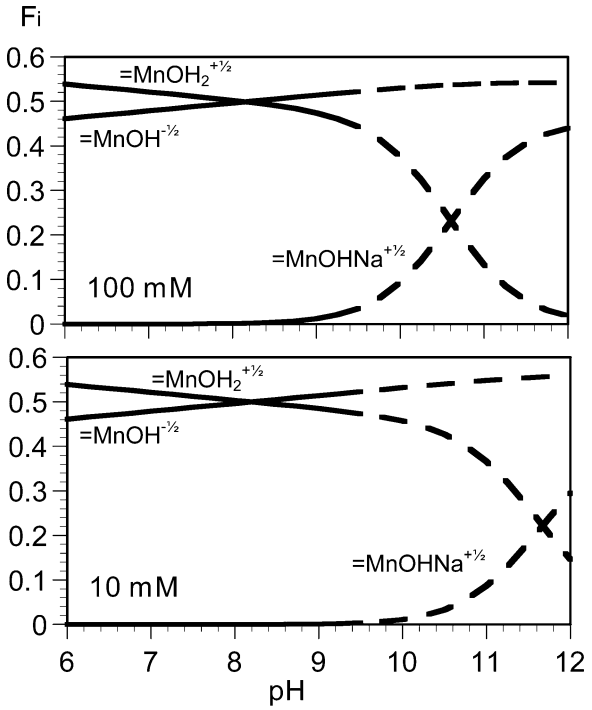

Figure 6. The speciation of manganite surface groups as a function of pH. The dashed lines represent an extrapolation of the model.

showing the model distribution of surface species are presented in Figure 6. Approximately 10% of the surface site concentration is found as the Na^+−surface complex at pH 10 in 100 mM NaCl. As expected, this complex is weak as indicated by (7).

$$\equiv MnOH^{-1/2} + Na^+ \rightleftharpoons \equiv MnOHNa^{+1/2} \qquad \log K(\text{intr.}) = -1.4 \quad (7)$$

This model is also supported by the XPS data, which shows a low affinity for Na^+ at the surface. For example, at pH = 10 the Na_{excess}/Mn ratio (cf. Figure 3) is approximately 0.05 in 10 mM NaCl.

It can be argued that the lack of ionic strength effects at low pH is due to the presence of SO_4^{2-} on the surface of the manganite, which would suppress the ionic strength effect. To check this, the dataset was fit using the BSM and introducing a sulfate surface complex according to (8).

$$\equiv MnOH_2^{+1/2} + SO_4^{2-} \rightleftharpoons \equiv MnOH_2^{+1/2}SO_4^{2-} \quad (8)$$

However, this model could not reproduce the loss of ionic strength at low pH and could not give a good fit to the experimental data. Thus, the presence of such a surface complex could not be supported by this dataset and at these low sulfate concentrations.

In the protonation/deprotonation reactions, only 9% of the crystallographic sites are proton active in the pH range studied here. This is much lower than previously published site activities for metal ion adsorption. For example, data for Cd(II) adsorption onto manganite[13] indicate that 8.9 μmol/m^2 Cd(II) adsorbs on manganite without any signs of Cd(II) hydroxide precipitation or polymerization. If the dominating crystal plane of manganite is assumed to be (010), this would correspond to 68% of the crystallographic sites. Comparable adsorption capacities were also found for Pb(II) by Matocha et al.[12] In their study, it was found that approximately 33% of crystallographic sites are occupied by Pb^{2+} with no indication of hydroxide precipitation.

This difference between the proton adsorption capacity and the capacity to adsorb metal ions suggests that it is difficult to protonate/deprotonate the basal planes of the manganite surface in the pH range between 6 and 9 but that metal ions still interact strongly with the manganite surface. Spectroscopic and thermodynamic studies are in progress to investigate these interactions with and without the presence of small organic ligands, and this work will be published soon.

Conclusions

The manganite studied in this work exhibits a very low buffering capacity between pH 6 and 9. The surface has a net positive charge at pH below 8.2 which is the pH_{iep}. This pH_{iep} is also equal to the potentiometrically determined pH_{nzpc}. The increased buffer capacity at pH > 8.2 suggests that Na^+ interacts with the surface. This hypothesis is supported by XPS measurements and by AcoustoSizer measurements and can be attributed to the formation of a complex between Na^+ from the ionic medium and a negatively charged surface site. At pH values between 6 and 8, manganite does not exhibit any of the characteristics that can be explained with ionic strength effects.

Acknowledgment. The authors acknowledge Johannes Lützenkirchen for adaptations in the Fiteql code and for valuable discussions. Staffan Wall and Mikael Rasmusson, Physical Chemistry, Gothenburg University, are acknowledged for the use of the AcoustoSizer and for help during these measurements, and John Loring is acknowledged for linguistic corrections. The Swedish Research Council is acknowledged for financial support.

LA0496338